Electronic Supplementary Material (ESI) for RSC Advances.

Synthesis and self-assembly of a penta[60]fullerene bearing benzo[ghi]perylenetriimide units

Clément Drou,[a] Théo Merland,[b] Antoine Busseau,[a] Sylvie Dabos-Seignon,[a] Antoine Goujon,[a] Piétrick Hudhomme,[a] Lazhar Benyahia,[b] Christophe Chassenieux,*[,b] Stéphanie Legoupy*[,a]

a. Laboratoire MOLTECH-Anjou, UMR CNRS 6200, UNIV Angers, SFR MATRIX, 2 Bd Lavoisier, 49045 Angers Cedex, France.

b. Institut des Molécules et Matériaux du Mans, UMR CNRS 6283, Le Mans UNIV, 1, Av Olivier Messiaen, 72085 Le Mans Cedex 9, France

Table of contents

General

NMR ^{1}H, ^{1}H-COSY and DOSY spectra were recorded using Bruker 300 MHz Avance III and ^{13}C spectra were recorded at 125 MHz on a Bruker 500 MHz Advance III HD spectrometers. Chemical shifts were reported in ppm according to tetramethylsilane using the solvent residual signal as an internal reference ($CDCl_3$: δ_H = 7.26 ppm and δ_C = 77.16 ppm).

MALDI-TOF spectra were performed on a Spiral TOF JMS-S3000 using DCTB (trans-2-[3-(4-tert-Butylphenyl)-2-methyl-2-propenylidene]malononitrile) as matrix.

HPLC analyses were performed on a Shimadzu CBM-20A controller equipped with a Buckyprep Waters (4.6 x 250 mm) column and a Shimadzu SPD-M20A photodiode array detector at 40°C.

UV-visible absorption spectra were recorded on a Shimadzu UV-1800 spectrophotometer.

Cyclic voltamperograms (CV) were recorded on a potentiostat SP 150 (Bio-Logic) monitored by EC-Lab software. All the electrochemical measurements were achieved in glovebox using a glassy carbon working electrode and a Pt wire as counter electrode. CV were carried out at a scan rate of 100 $mV.s^{-1}$ with Bu_4NPF_6 0.1 M as supporting electrolyte.

Atomic Force Microscopy (AFM) studies were completed using the Nano-Observer microscope (CSInstruments) under ambient conditions (room T°, pressure and air). The obtained images were processed with the open access sotfware Gwyddion. Solutions of compounds **5** or **6** were prepared in $CHCl_3$ at various concentrations (200 µM, 400 µM and 600 µM) and then spin coated on a glass substrate.

Light Scattering measurements were recorded at 20°C and at scattering angles θ ranging from 30° up to 150° with a CGS-3 compact system equipped with an LSE-5004 correlator from ALV GmbH, Germany in combination with a He-Ne laser at a fixed wavelength (λ) of 632.8 nm.

Static Light Scattering (SLS) results were expressed in terms of Rayleigh ratios $R(\theta)$ calculated according to:

$$R(\theta) = \frac{I_{solution} - I_{solvent}}{I_{standard}} \times R(\theta)_{standard} \quad \text{Eq. S1}$$

with I_i the scattered intensities where i stands for the solution, the solvent (chloroform) or the standard (toluene for which $R(\theta)_{standard} = 1.35.10^{-5}$ cm^{-1}).

Note that the intensity scattered by the solutions of compounds **4** and **5** has been corrected from the absorption at λ as suggested by Ref.S1. The experiments window scale in length was defined by the scattering wave vector whose magnitude q is given in m^{-1} according to:

$$q = \frac{4n\pi}{\lambda} sin(\frac{\theta}{2}) \quad \text{Eq. S2}$$

with n the refractive index of solvent. Here q varies from $7.4.10^6$ up to $2.8.10^7$ m^{-1}. In this study, there was no angular dependence of $R(\theta)$ over the q range investigated which meant that the scattering species in solution were small. The values of R which are displayed in Figure 4 correspond then to averages of $R(\theta)$ over θ. $R(\theta)$ is related to the weight average molar mass of the scatterers (M_w) according to the Zimm equation:

$$\frac{KC}{R(\theta)} = \frac{1}{M_w}(1 + \frac{q^2 R_g{}^2}{3}) \quad \text{Eq. S3}$$

$$where\ K = \frac{4\pi^2 n_{ref}^2}{N_{Av}\lambda^4}(\frac{\partial n}{\partial c})^2 \quad \text{Eq. S4}$$

with C the concentration of solute, N_{Av} the Avogadro number, n_{ref} the refractive index of the standard, dn/dC the specific refractive index increment which is related to the contrast of the scattering species with respect to the solvent and R_g, the radius of gyration of the scatterers. Here, as already explained, solutions of compounds **4**, **5** and **6** in chloroform display no angular dependence of their scattering intensities which meant that R_g was smaller than 20nm and the term $q^2R_g{}^2/3$ can be neglected.

Solutions of compound **4** and C_{60} in chloroform scattered the same intensity as their solvent which meant that the dn/dC of C_{60} and of **4** in this solvent are almost equal to zero. Solutions of compounds **5** and **6** in chloroform scattered more than chloroform, therefore the contrast originated from BPTI moieties.

Dynamic light scattering (DLS) measurements focus on the fluctuations of scattered intensity. These fluctuations are related to the diffusion of the solute and their characteristic relaxation times τ(q) are related the size of the scatterers. DLS measured the intensity autocorrelation functions $g_2(q,t)$ that were converted to electrical field correlation functions $g_1(q,t)$ thanks to Siegert equation[S2]:

$$g_2(q,t) = 1 + \beta|g_1(q,t)|^2 \quad \text{Eq. S5}$$

with β the intercept. For every solution of compound **5** in chloroform, only one symmetric relaxation mode was observed and $g_1(q,t)$ functions measured at a given value of q were fitted with continuous distributions of the relaxation times (see figure S26) with the following equation [S2]:

$$g_1(q,t) = \int A(\tau)\exp\left(-\frac{t}{\tau}\right)dt \quad \text{Eq. S6}$$

Solutions for compounds **4** and **6** in chloroform did not display any autocorrelation function, because of the small size of the scatterers and the low contrast, respectively.

For solutions of compound **5** in chloroform, the relaxation times are q^{-2} dependent (see Figure S27) which meant that a diffusive motion was probed. The cooperative diffusion coefficients D_c were then computed according to :

$$D_c = \frac{1}{\tau q^2} \quad \text{Eq. S7}$$

Hydrodynamic radii r were calculated using the Stokes-Einstein equation :

$$r = \frac{kT}{6\pi\eta_s D_i} \quad \text{Eq. S8}$$

where k is the Boltzmann constant, T the temperature of measurement in (equal to 293 K for DLS and 298 K for DOSY NMR), η_s the solvent viscosity at temperature T.

Analysis

NMR Spectra

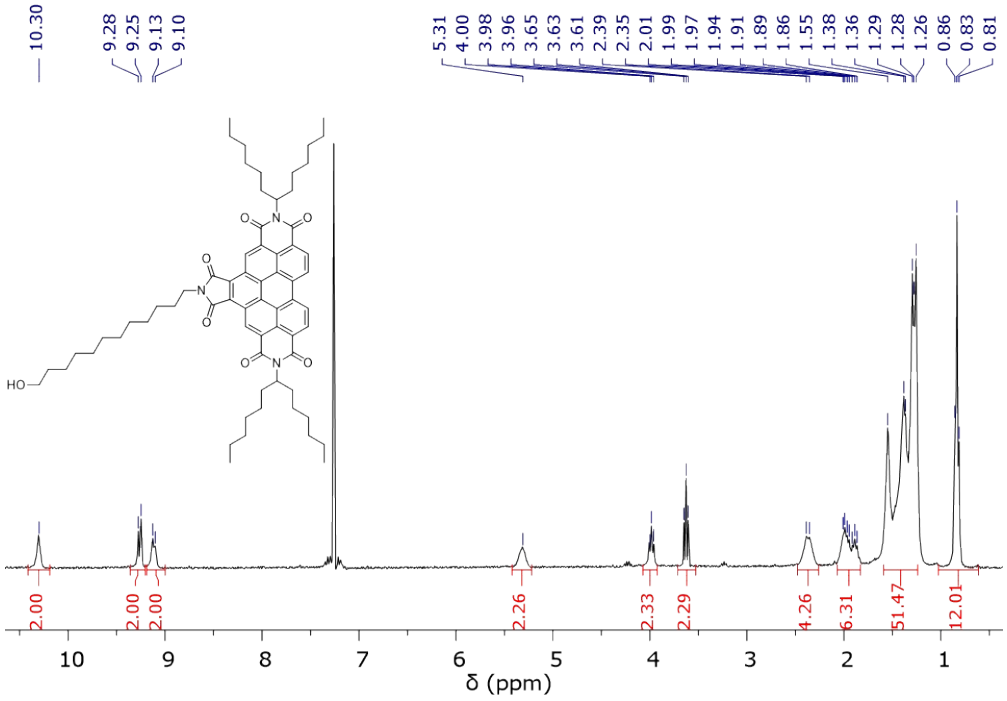

Figure S1. ^{1}H NMR spectrum (300 MHz, $CDCl_3$) of compound **2**.

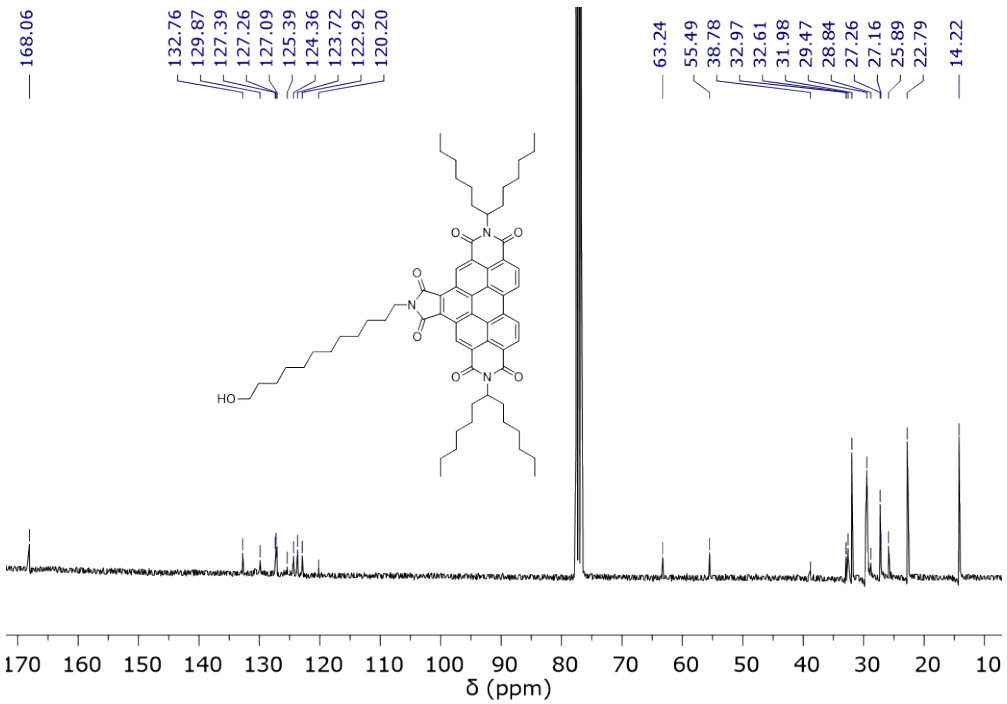

Figure S2. ^{13}C NMR spectrum (125 MHz, $CDCl_3$) of compound **2**.

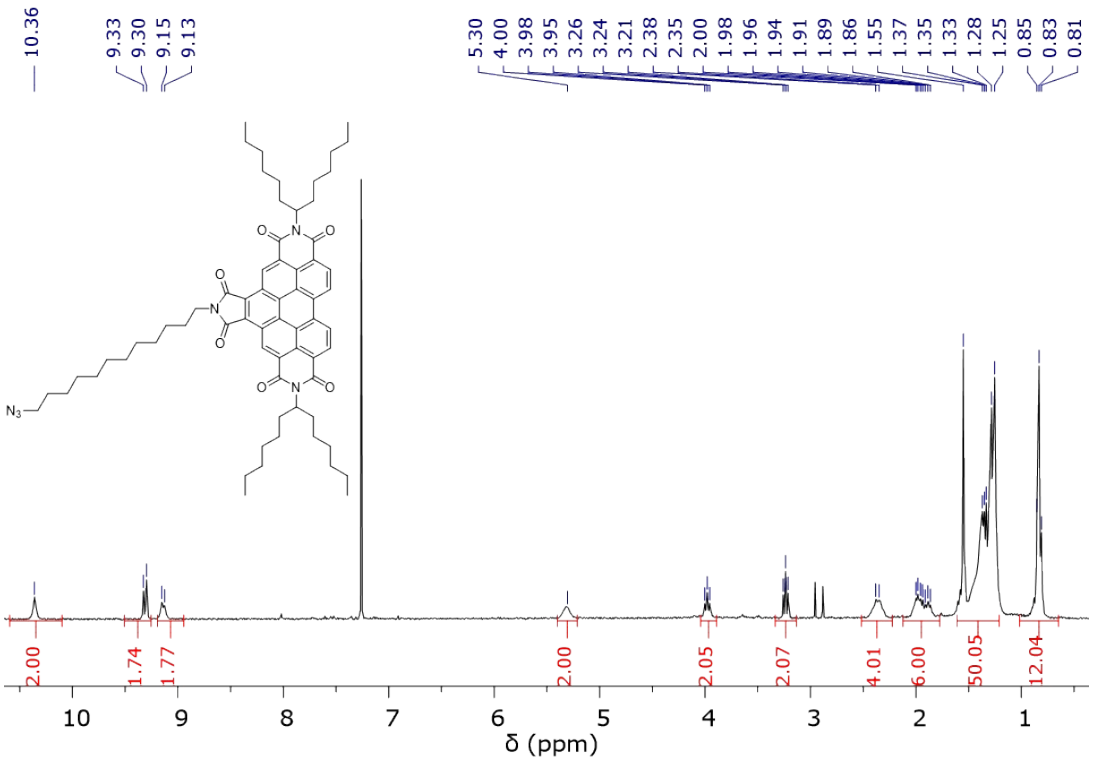

Figure S3. ^{1}H NMR spectrum (300 MHz, $CDCl_3$) of compound **3**.

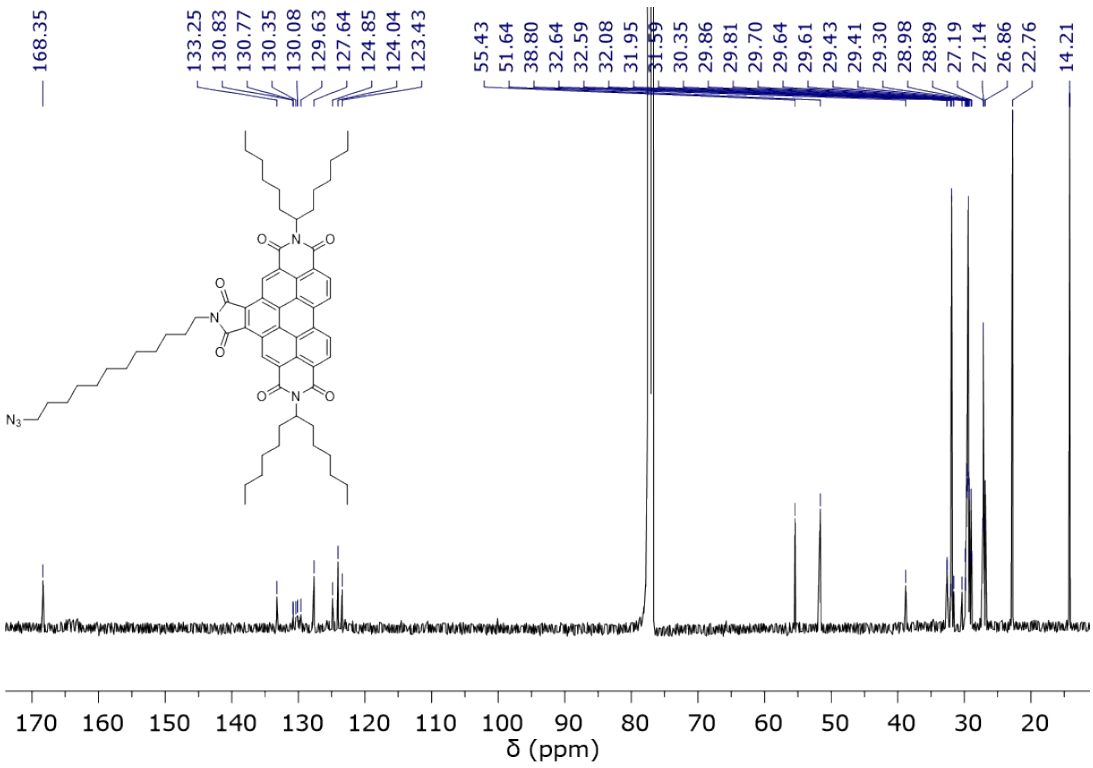

Figure S4. ^{13}C NMR spectrum (125 MHz, $CDCl_3$) of compound **3**.

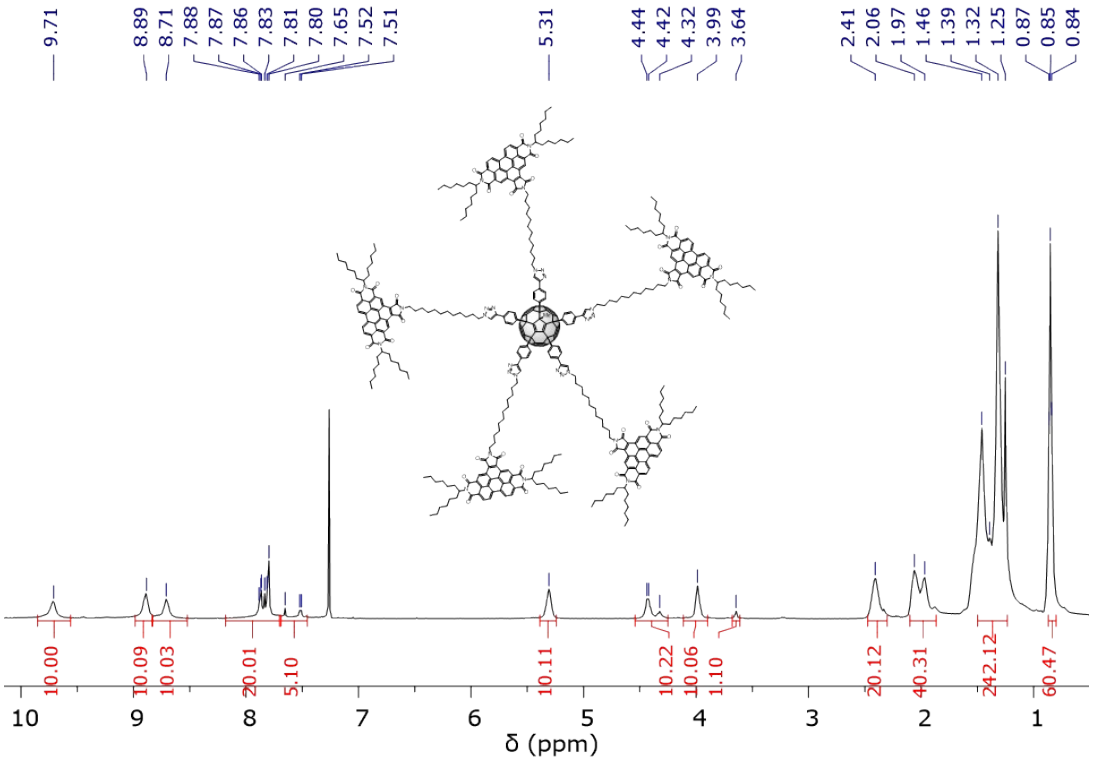

Figure S5. ^{1}H NMR spectrum (300 MHz, $CDCl_3$) of penta(BPTI)[60]fullerene **5**.

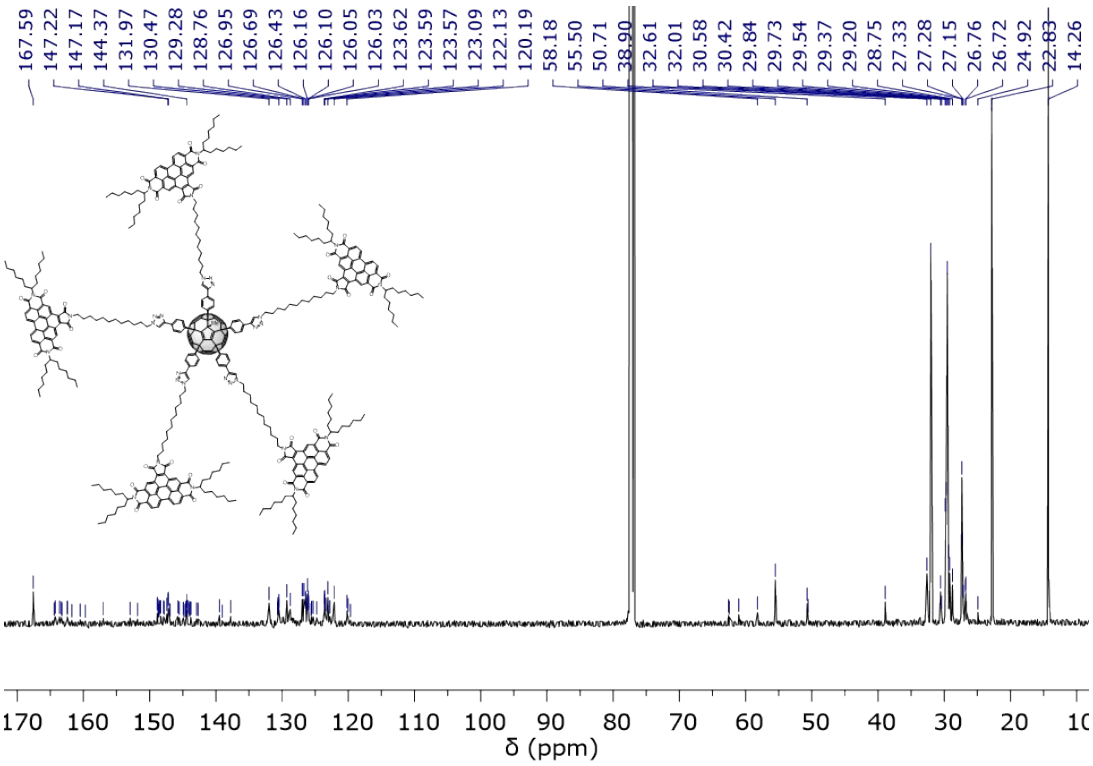

Figure S6. ^{13}C NMR spectrum (125 MHz, $CDCl_3$) of penta(BPTI)[60]fullerene **5**.

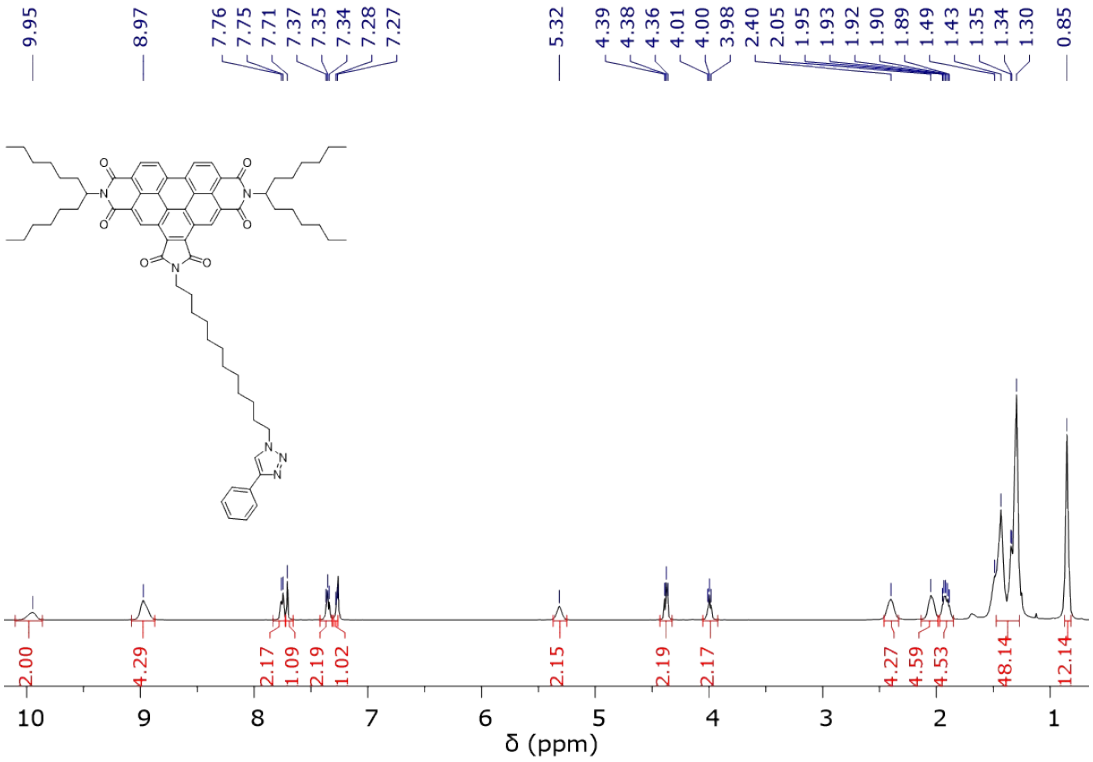

Figure S7. ^{1}H NMR spectrum (300 MHz, $CDCl_3$) of reference **6**.

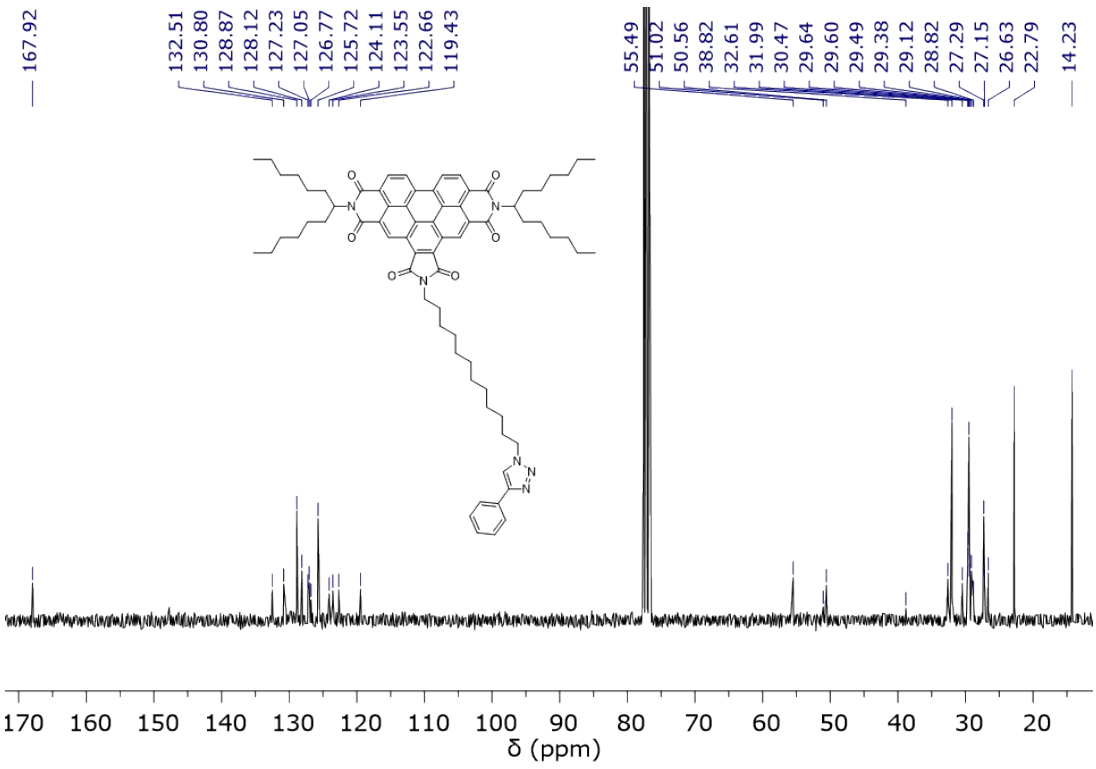

Figure S8. ^{13}C NMR spectrum (125 MHz, $CDCl_3$) of reference **6**.

a)

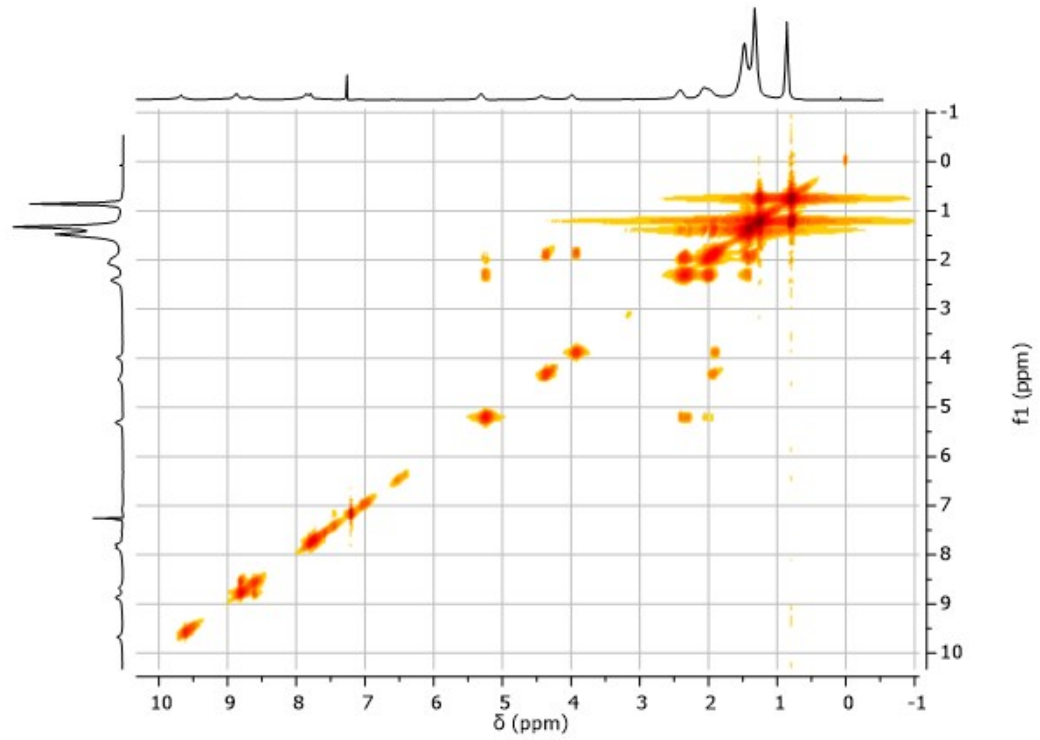

b)

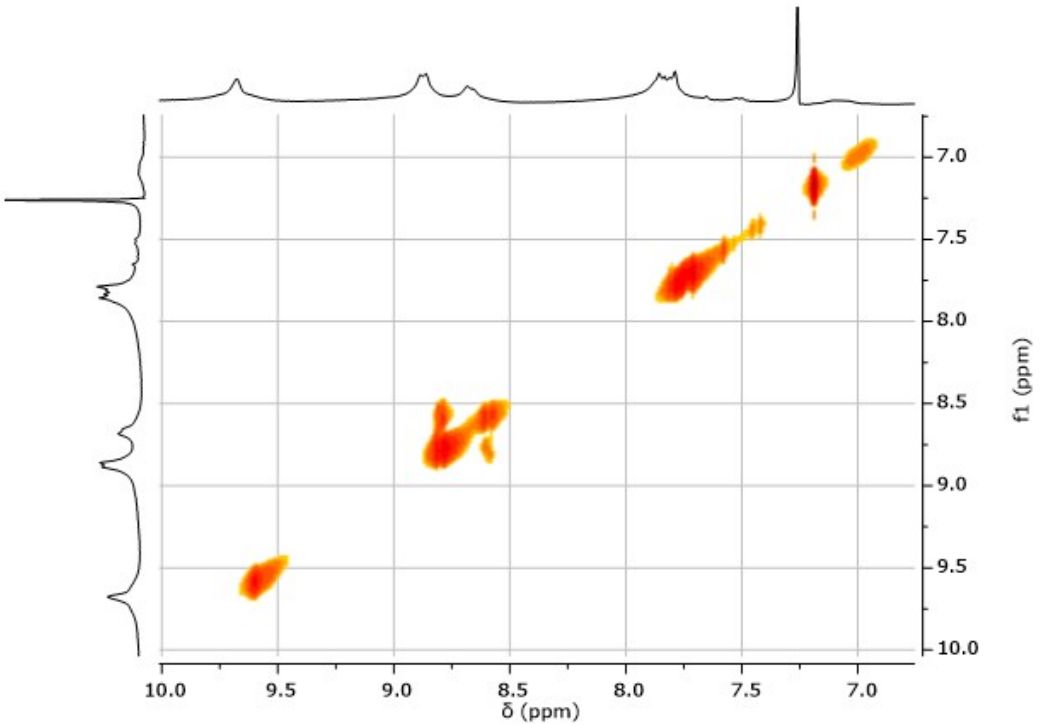

Figure S9. ^{1}H-COSY NMR spectra (300 MHz, $CDCl_3$, 298 K) of penta(BPTI)[60]fullerene **5**, a) full spectrum and b) aromatic region.

a)

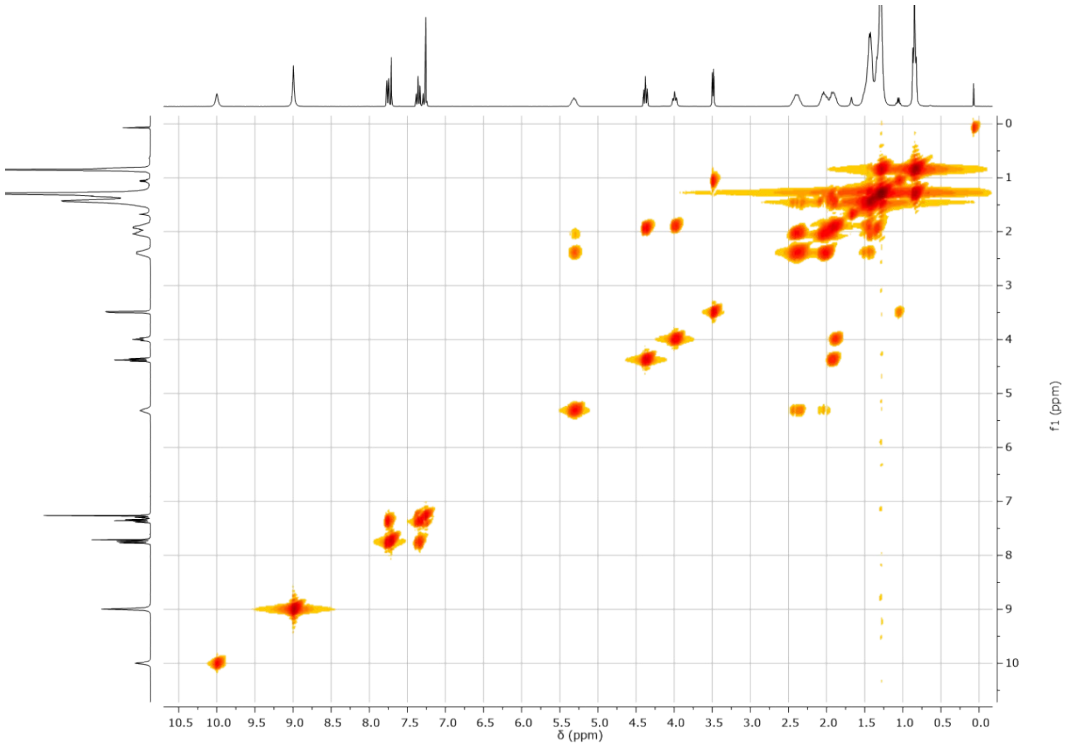
10.5 10.0 9.5 9.0 8.5 8.0 7.5 7.0 6.5 6.0 5.5 5.0 4.5 4.0 3.5 3.0 2.5 2.0 1.5 1.0 0.5 0.0
δ (ppm)
0 1 2 3 4 5 6 7 8 9 10
f1 (ppm)

b)

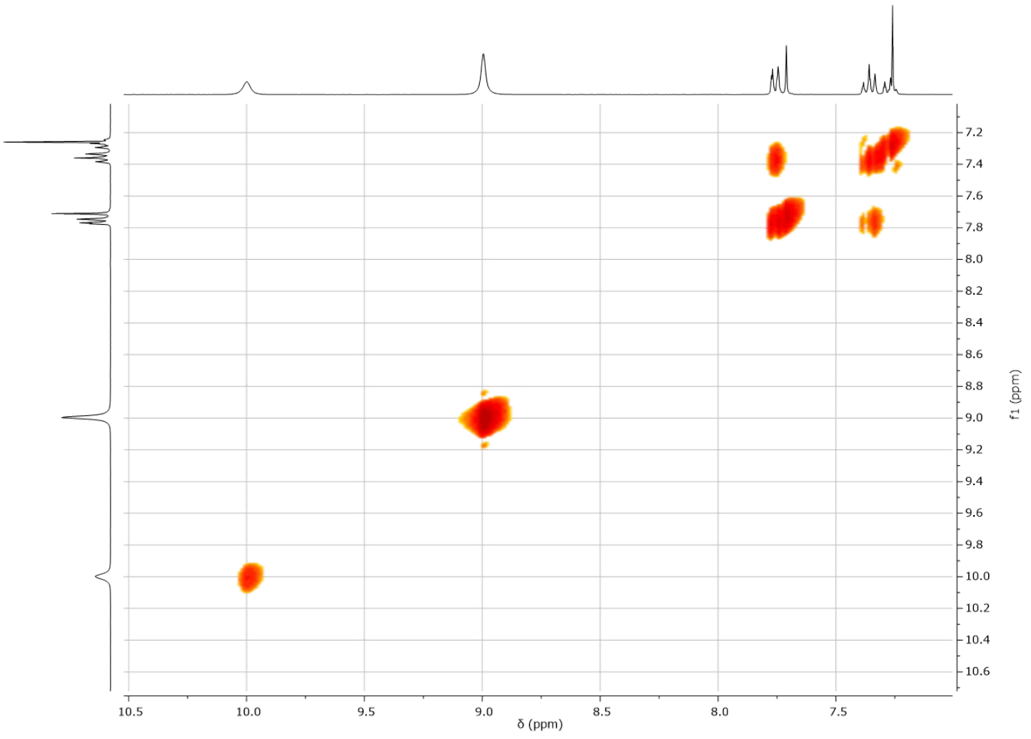
10.5 10.0 9.5 9.0 8.5 8.0 7.5
δ (ppm)
7.2 7.4 7.6 7.8 8.0 8.2 8.4 8.6 8.8 9.0 9.2 9.4 9.6 9.8 10.0 10.2 10.4 10.6
f1 (ppm)

Figure S10. ^{1}H-COSY NMR spectra (300 MHz, $CDCl_3$, 298 K) of reference **6**, a) full spectrum and b) aromatic region.

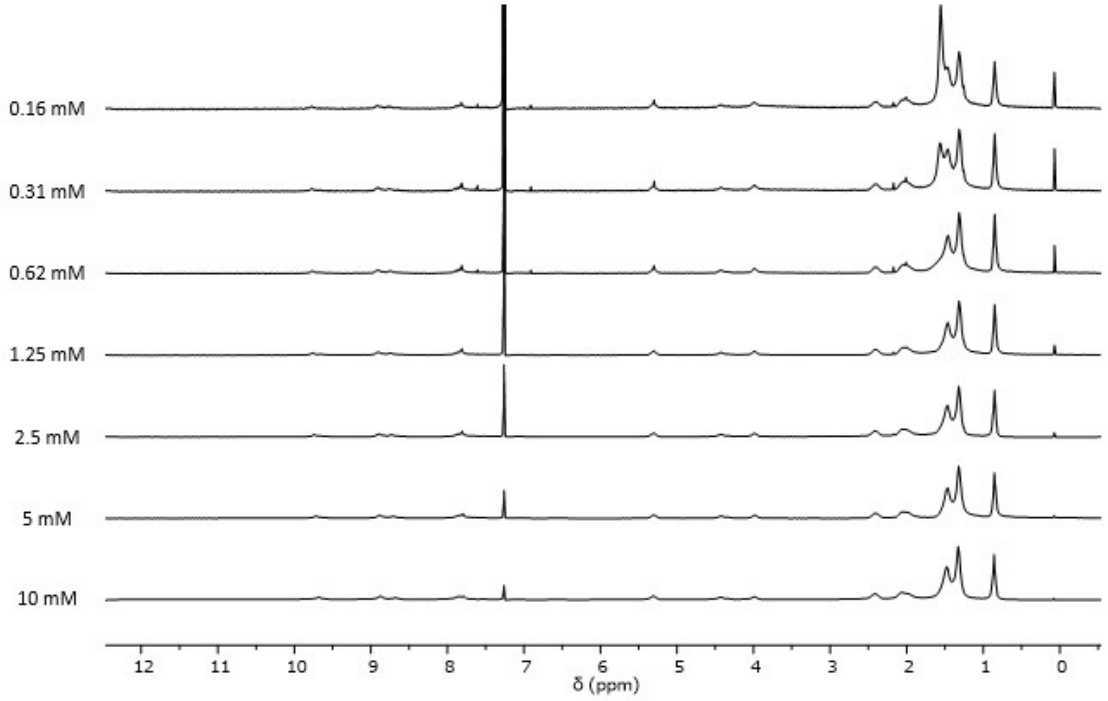

Figure S11. ^{1}H NMR spectrum (300 MHz, $CDCl_3$, 298 K) of penta(BPTI)[60]fullerene **5** at different concentrations (full spectrum).

a)

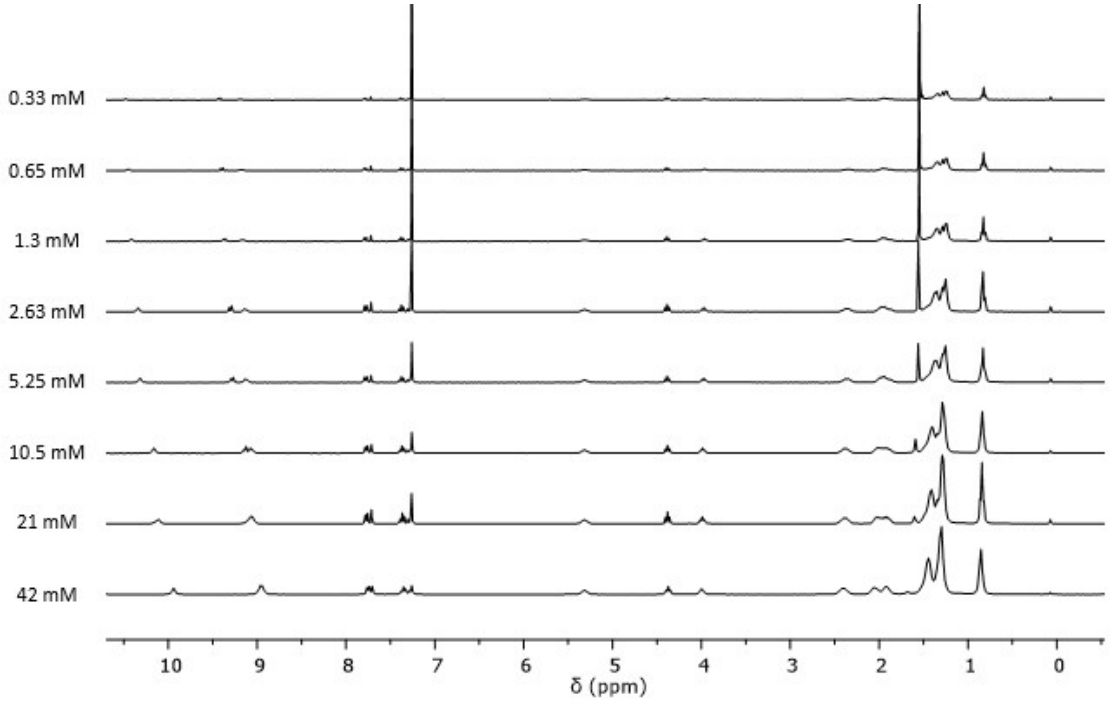

b)

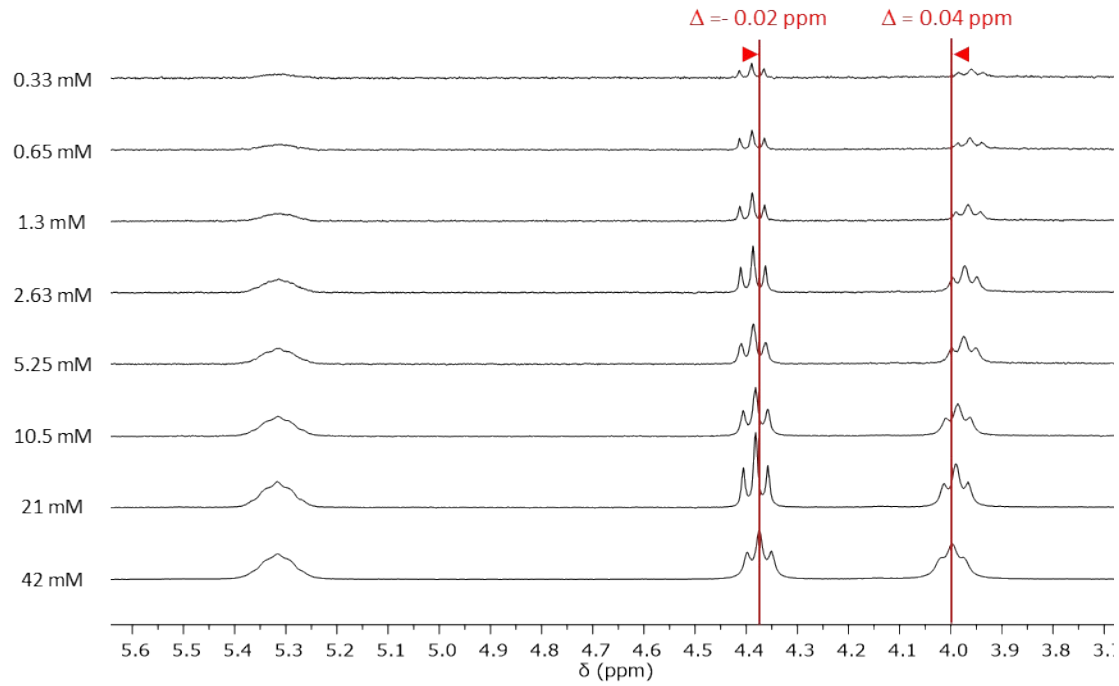

Figure S12. ^{1}H NMR spectrum (300 MHz, $CDCl_3$, 298 K) of reference **6** at different concentrations, a) full spectrum and b) triazole + aliphatic region.

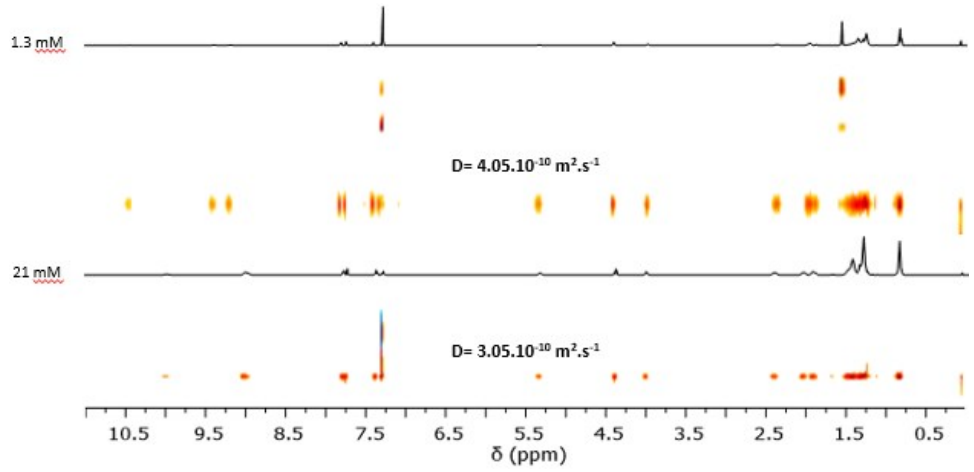

Figure S13. ^{1}H DOSY NMR spectrum (300 MHz, $CDCl_3$, 298 K) of reference **6** at different concentrations.

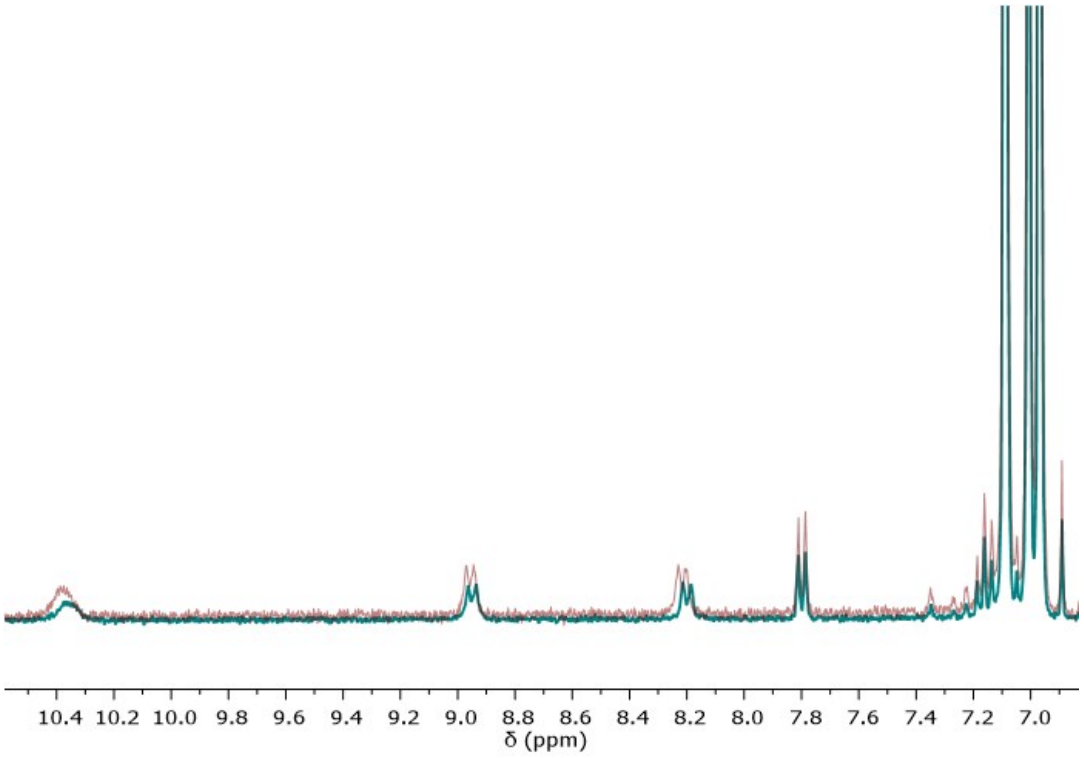

Figure S14. ^{1}H NMR spectrum (300 MHz, $CDCl_3$, 298 K) of reference **6** in green and reference **6** + C_{60} in red, magnified in aromatic region.

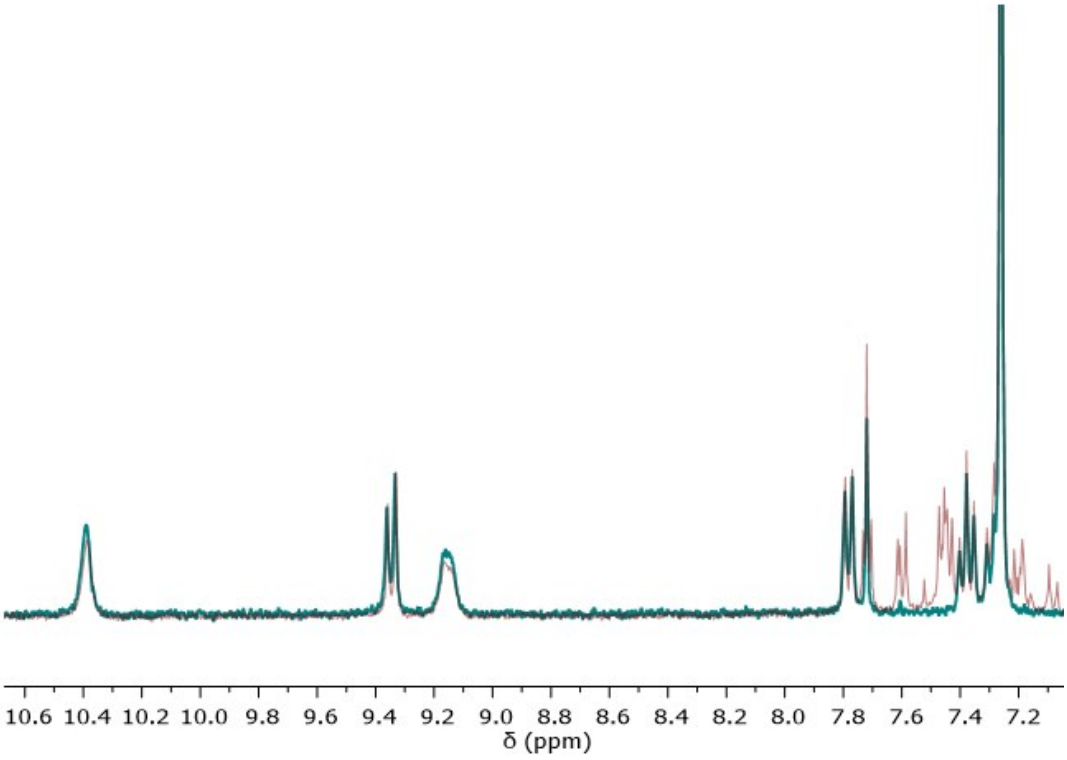

Figure S15. ^{1}H NMR spectrum (300 MHz, $CDCl_3$, 298 K) of reference **6** in green and compounds **4** + **6** in red, magnified in aromatic region.

Mass spectra

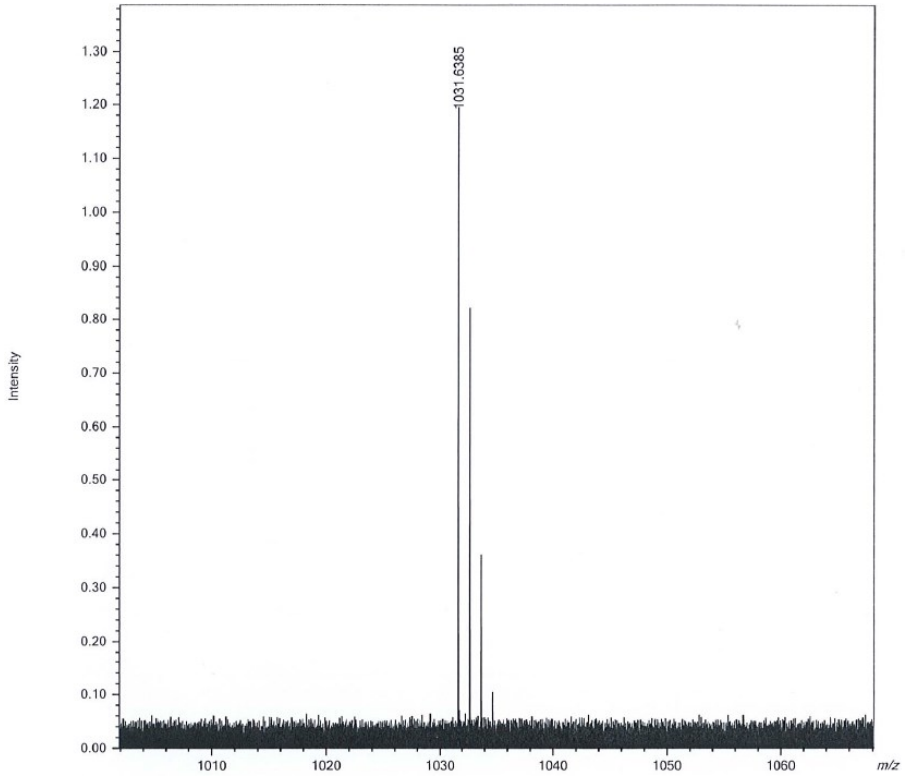

Figure S16. MALDI TOF HRMS spectrum of compound **2**.

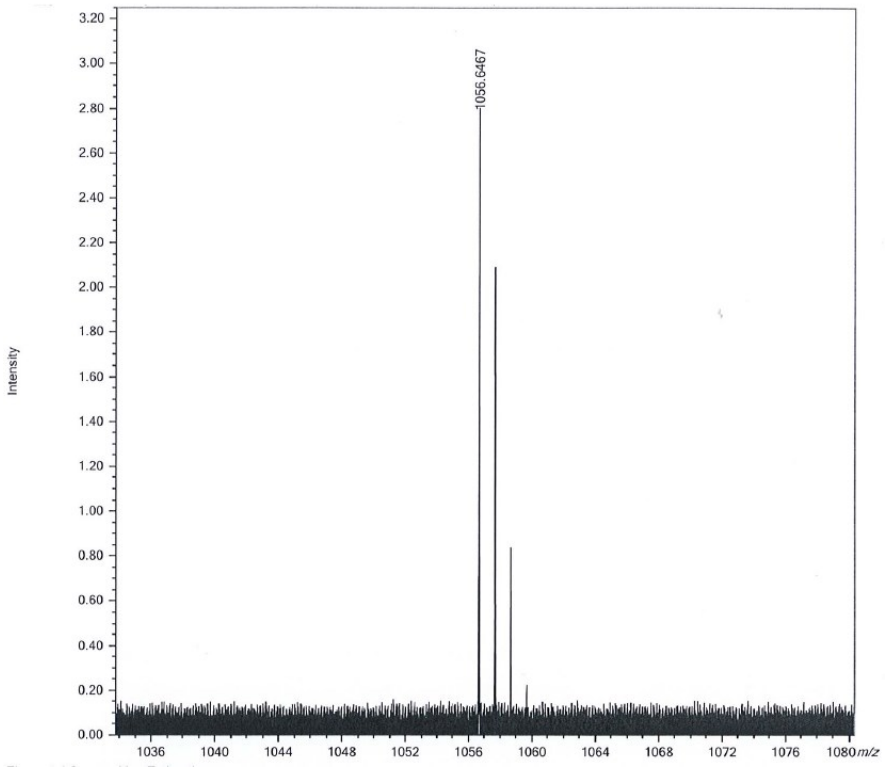

Figure S17. MALDI TOF HRMS spectrum of compound **3**.

a)

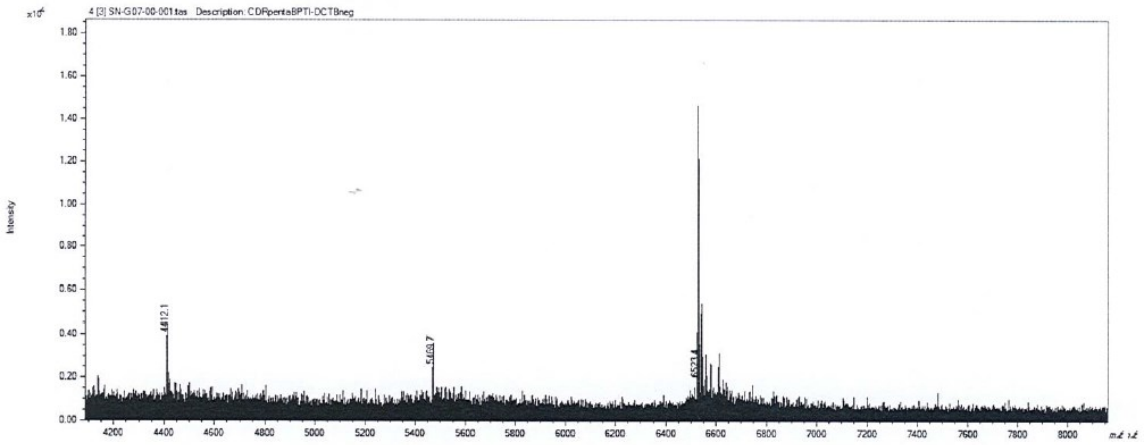

b)

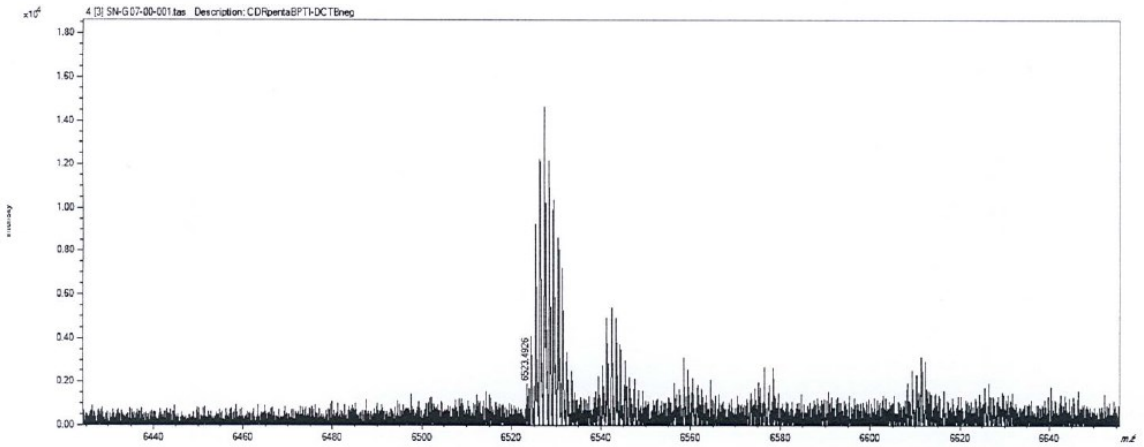

Figure S18. MALDI TOF HRMS spectrum of penta(BPTI)[60]fullerene **5**. a) region 4200-8000 m/z b) magnified in 6440-6640 m/z region.

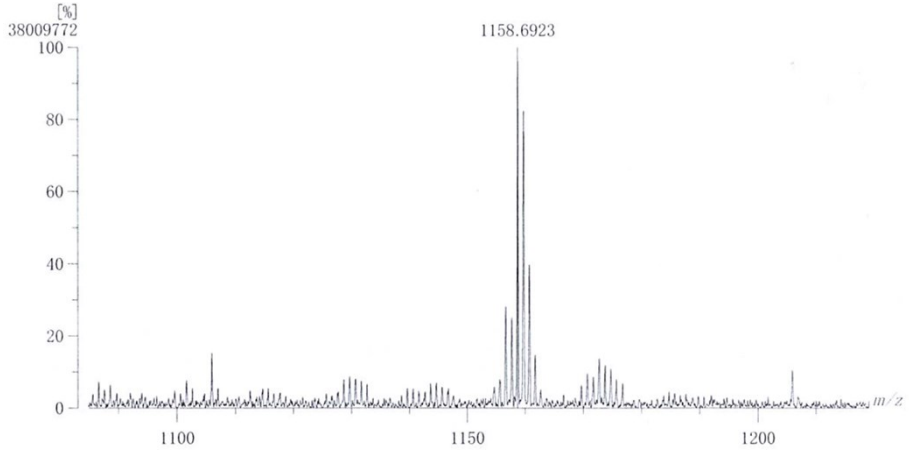

Figure S19. MALDI TOF HRMS spectrum of reference **6**.

HPLC Chromatograms

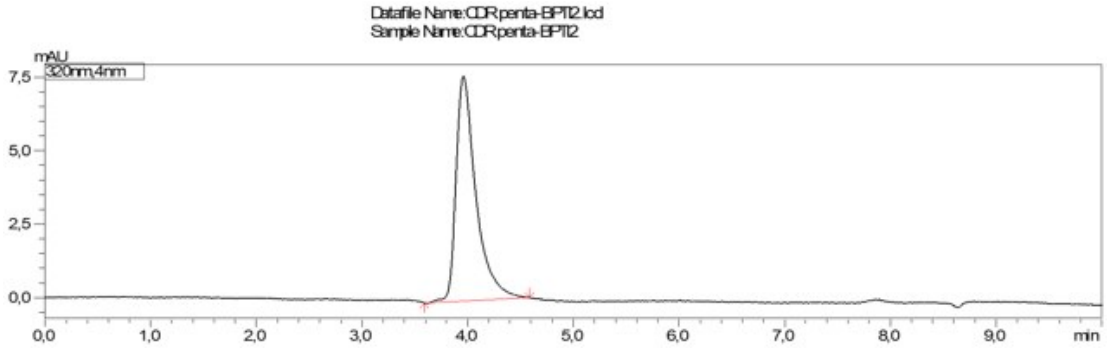

Figure S20. HPLC chromatogram of penta(BPTI)[60]fullerene **5**. Retention time: 3.96 min (eluent: toluene, flow rate: 1 mL/min, wavelength: 320 nm).

UV-visible absorption spectra

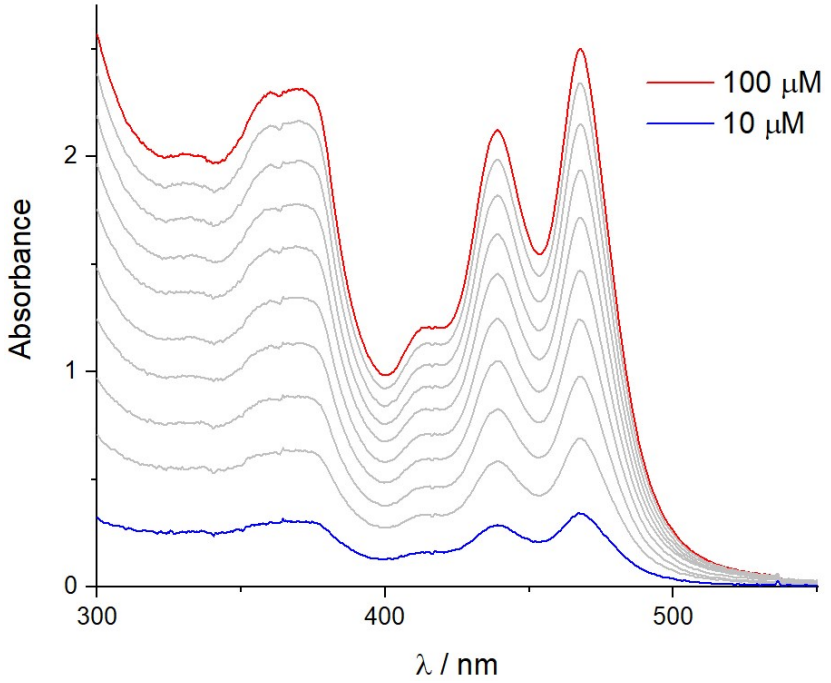

Figure S21. Absorption spectra of penta(BPTI)[60]fullerene **5** at different concentrations (10-100 μM, region 300-550 nm ($CHCl_3$, 298 K, 2 mm cuvette).

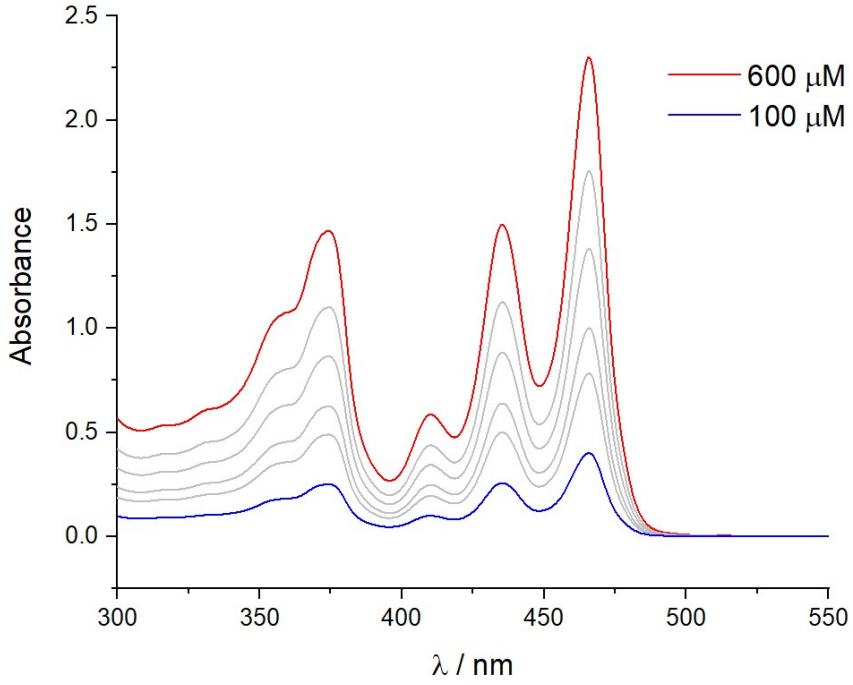

Figure S22. Absorption spectra of reference **6** at different concentrations (100-600 μM, region 300-550 nm ($CHCl_3$, 298 K, 2 mm cuvette).

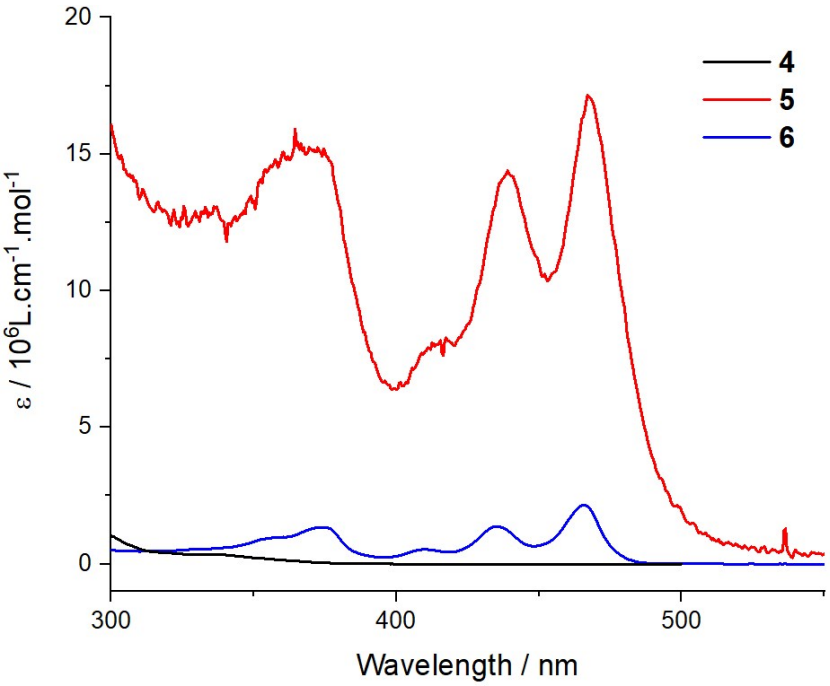

Figure S23. Absorption spectra of compounds **4**, **5** and **6** at 10 μM, region 300-600 nm ($CHCl_3$, 298 K, 1 cm cuvette).

Light scattering

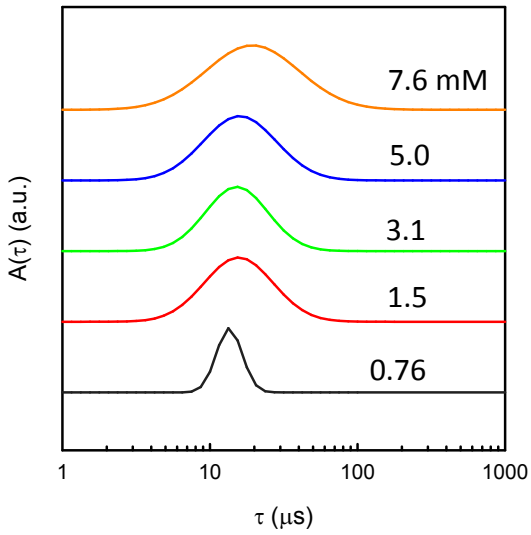

Figure S24. Distribution of relaxation times measured at θ=150° for various concentrations of penta(BPTI)[60]fullerene **5** in chloroform as labelled on the figure. For each concentration curves have been shifted vertically by an arbitrary constant to make the comparison clearer.

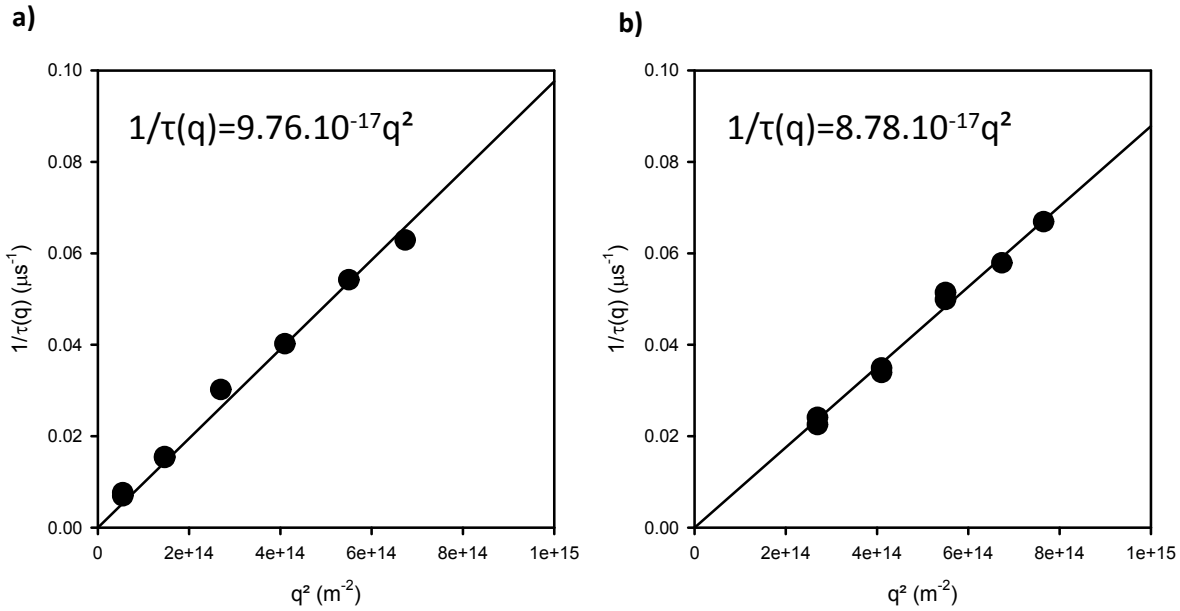

Figure S25. Variation of the relaxation time with q^2 for solutions of penta(BPTI)[60]fullerene **5** in chloroform at 1.5 mM (a) and 5.0 mM (b). Diffusions coefficients D_c (in $m^2/\mu s$) correspond to the slopes of a linear regression (solid line) of the data.

Cyclic voltammograms

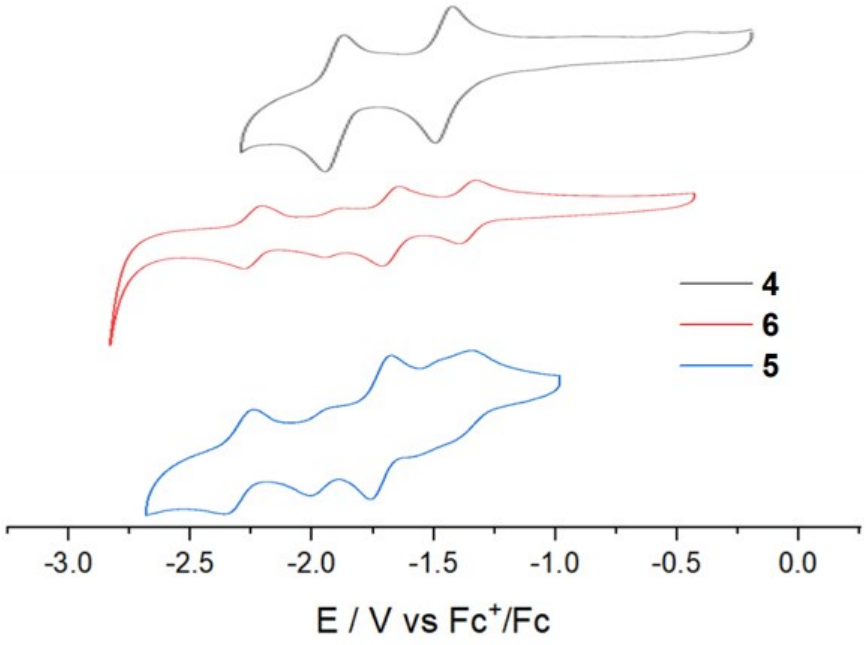

Figure S26. Cyclic voltammograms of compound **4** ($7.3.10^{-4}$ M), penta(BPTI)[60]fullerene **5** (10^{-4} M) and reference **6** ($5.\ 10^{-4}$ M) (V vs Fc^+/Fc ; WE: glassy carbon ; Bu_4NPF_6 0.1 M as supporting electrolyte; 100 $mV.s^{-1}$; ODCB/MeCN 4:1 ; 298 K).

Compound	E^1_{Red}[a]	E^2_{Red}[b]	E^3_{Red}[a]	E^4_{Red}[b]	E^5_{Red}[a]
4	-	-1.94	-	-1.49	-
6	-2.27	-	-1.70	-	-1.38
5	-2.35	-2	-1.75	overlap	overlap

[a]Reduction potential of BPTI.

[b]Reduction potential of fullerene.

Table S1. Reduction potentials of compounds **4**, **5** and **6** (V vs Fc^+/Fc ; WE: glassy carbon ; Bu_4NPF_6 0.1 M as supporting electrolyte; 100 $mV.s^{-1}$; ODCB/MeCN 4:1 ; 298 K).

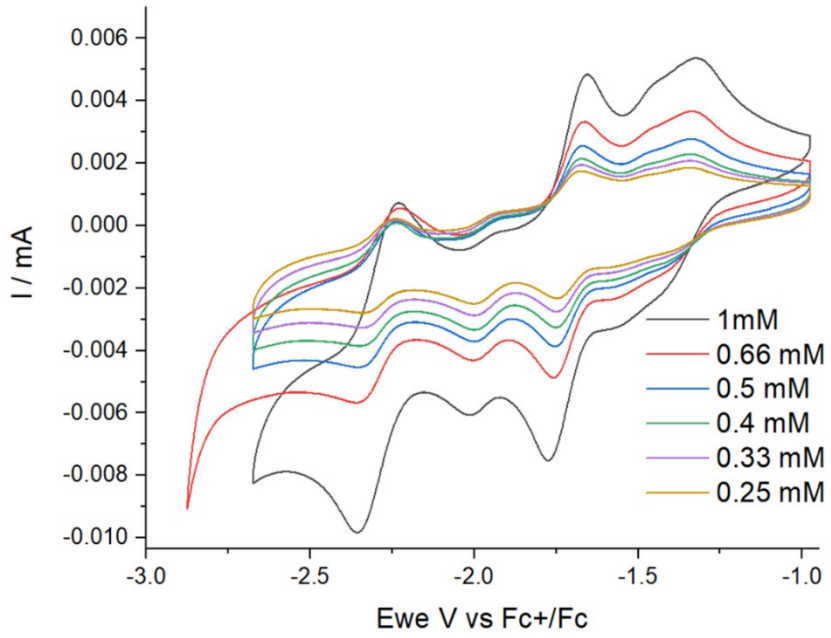

Figure S27. Cyclic voltammograms of penta(BPTI)[60]fullerene **5** at different concentrations (V vs Fc^+/Fc ; WE: glassy carbon ; Bu_4NPF_6 0.1 M as supporting electrolyte; 100 $mV.s^{-1}$; ODCB/MeCN 4:1 ; 298 K).

Concentration of 5	E^1_{Red}[a]	E^2_{Red}[b]	E^3_{Red}[a]
1 mM	-2.36	-2.01	-1.77
0.66 mM	-2.35	-2.00	-1.76
0.5 mM	-2.35	-2.00	-1.75
0.4 mM	-2.34	-2.00	-1.74
0.33 mM	-2.33	-1.99	-1.74
0.25 mM	-2.33	-1.99	-1.74

[a]Reduction potential of BPTI.
[b]Reduction potential of fullerene.

Table S2. Reduction potentials of penta(BPTI)[60]fullerene **5** at different concentrations (V vs Fc^+/Fc ; WE: glassy carbon ; Bu_4NPF_6 0.1 M as supporting electrolyte; 100 $mV.s^{-1}$; ODCB/MeCN 4:1 ; 298 K).

AFM images

a)

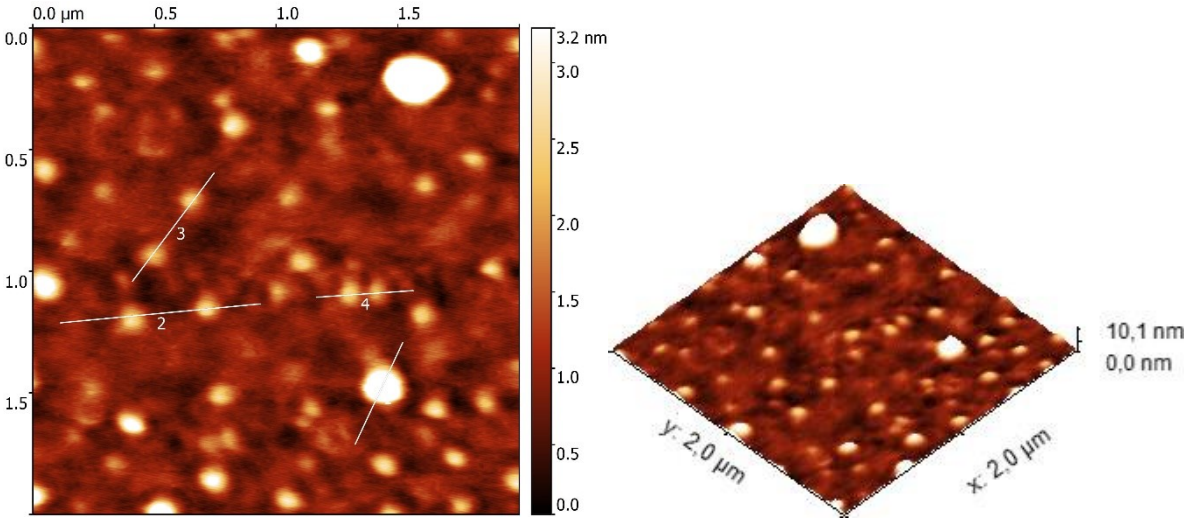

b)

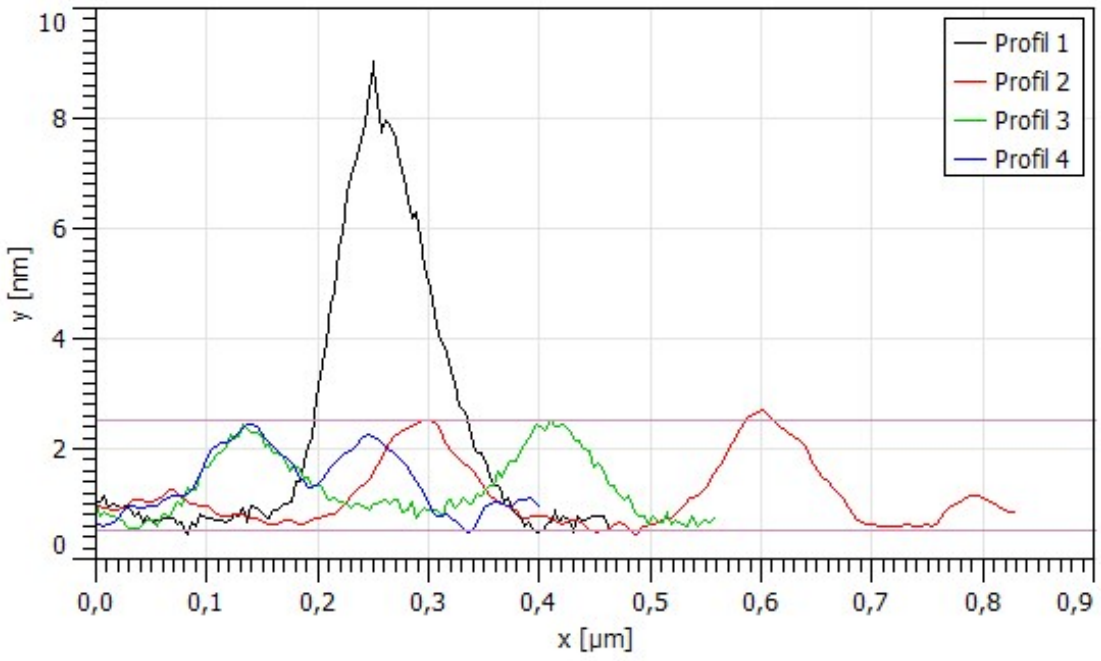

Heights : small aggregates : average of 2nm ; big aggragates : 9 nm

Figure S28. a) AFM images of penta(BPTI)[60]fullerene **5** in 2D and 3D from the 0.2 mM solution, spin coated onto glass substrate; b) - associated profiles.

a)

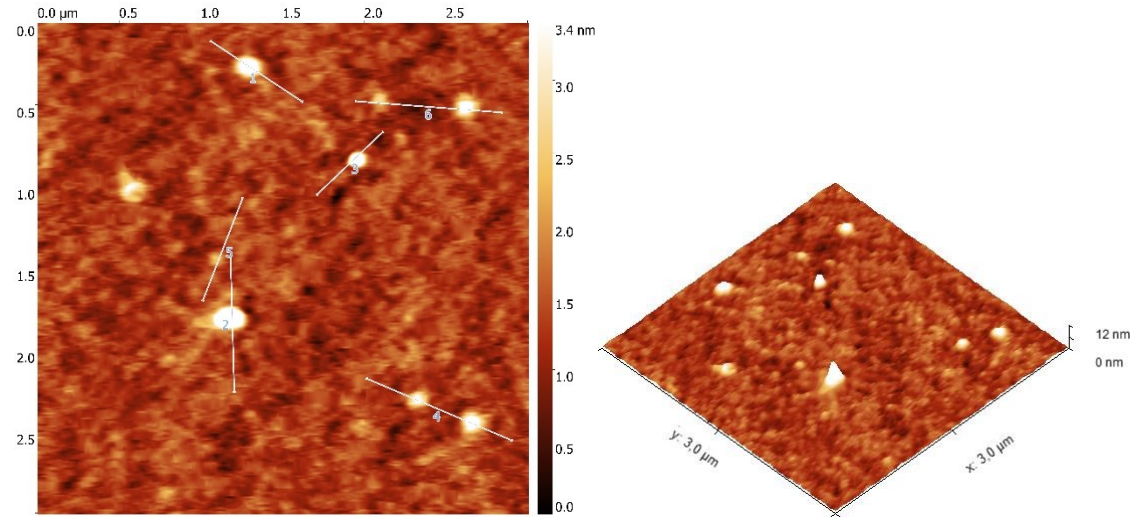

b)

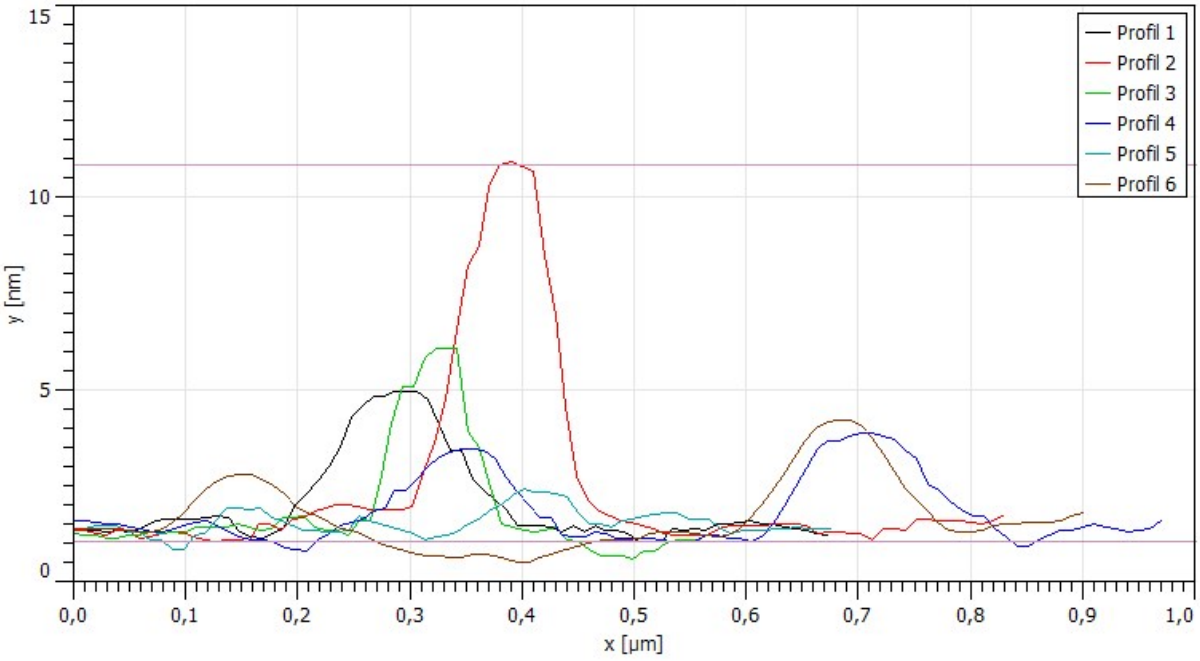

Heights of aggregates ranging from 2 nm up to 10 nm

Figure S29. a) AFM images of penta(BPTI)[60]fullerene **5** in 2D and 3D from the 0.6 mM solution, spin coated onto glass substrate; b) - associated profiles.

a)

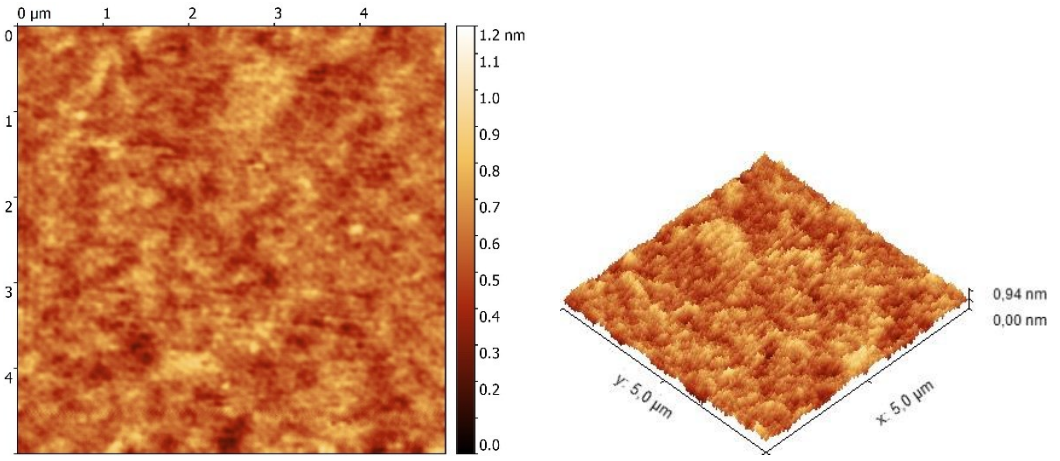

b)

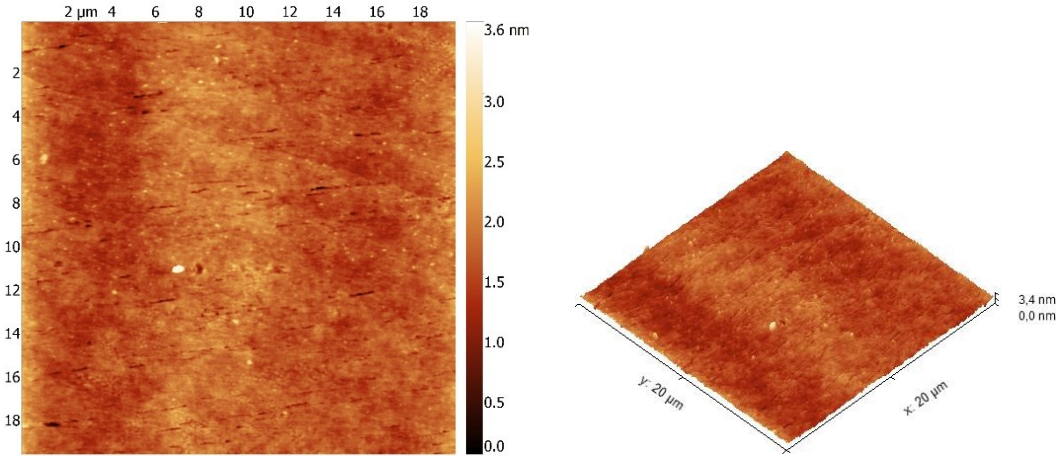

Figure S30. AFM scan of reference **6** spin coated on glass substrate at 0.2 mM, 2D and 3D view a) 5 µm x 5 µm and b) 20 µm x 20 µm.

References

(S1) T. Toupance, H. Benoit, D. Sarazin and J. Simon, *Journal of the American Chemical Society*, 1997, **119**, 9191–9197.

(S2) B. J. Berne and R. Pecora, *Science*, 1976, **194**, 1155–1156.